Regenerative Braking Control for Trains in a DC MicroGrid Using Dynamic Feedback Linearization Techniques

Filipe J. Perez, Alessio Iovine, Gilney Damm, Lilia Galai-Dol, Paulo Ribeiro

Regenerative Braking Control for Trains in a DC MicroGrid Using Dynamic Feedback Linearization Techniques

Filipe Perez [*,****] **Alessio Iovine** [**] **Gilney Damm** [***]
Lilia Galai-Dol [**] **Paulo Ribeiro** [****]

[*] *L2S Laboratory, Ecole CentraleSupelec, 3 rue Joliot-Curie, 91192 Gif-sur-Yvette, France (e-mail:filipe.perez@l2s.centralesupelec.fr)*
[**] *Efficacity, R&D Center, Paris, France, (e-mail: alessio.iovine@ieee.org, l.galai-dol@efficacity.com)*
[***] *IBISC Laboratory, Universite dEvry-Val dEssonne, 40 rue du Pelvoux, 91020 Evry, France (e-mail: gilney.damm@ibisc.fr)*
[****] *ISEE Institute, Federal University of Itajuba, 1303 Avenida BPS, 37500 903, Itajuba, Brazil (e-mail: aslan1952@gmail.com)*

Abstract: This paper proposes the integration of a train line for regenerative braking into a DC MicroGrid composed of PV generation, hybrid energy storage system (battery and supercapacitor) and DC local load. The energy generated from regenerative braking is absorbed by the supercapacitor, which is able to deal with bursts of power without affecting the stability of the system. The control scheme is based on singular perturbation analysis, where we can split the overall system in two interconnected subsystems with different time-scales dynamics, solving the non-minimal phase problem for DC/DC converters. Therefore, a simplified control strategy is obtained to control the train's converter and to assure stability of the whole MicroGrid. Simulation results show that the proposed control strategy can integrate regenerative braking from train as a renewable source in the MicroGrid.

Keywords: MicroGrids, Singular Perturbation, Dynamical Feedback Linearization.

1. INTRODUCTION

The modernization of power network known as SmartGrids is changing the way electrical power systems are designed. The efforts to reduce fossil based sources have brought high penetration of renewable energy sources (renewables) into the grid, with their intermittent and non-dispatchable characteristics. Also, the continuing electric load growth along with modern loads based on power electronics highlight the necessity to bring reliable solutions to improve power system operation (see Ribeiro et al. (2001, 2012)).

Direct Current (DC) MicroGrids are a good solution to better integrate renewables and reduce the impact of modern load applying a reliable operation that optimize the power flow in the grid, properly supplying the loads and guarantying power quality. The challenge here is to develop a control strategy that assures system stability, balancing the energy consumption and production in the grid (see Olivares et al. (2014)).

In this context, many transportation systems like electric vehicles and trains can be integrated in the MicroGrid system, generating a great impacts to it. For example, the regenerative braking of train cause bursts of power into the system in few seconds, bringing instability problems. Usually, classical linear PI control is not able to guarantee the operation of the system with this type of disturbance, even though it is widespread in the industry. Therefore, a rigorous stability study using nonlinear techniques in MicroGrids integrating transportation systems is more relevant towards SmartGrids issues (see Hernandez and Sutil (2016); Lu et al. (2014)).

This paper develops a control algorithm for bidirectional boost converters used to control the integration of regenerative braking from a train line into a DC MicroGrid, while considering stability of the whole MicroGrid. The DC MicroGrid is composed of a PV generation, two energy storage systems, a supercapacitor and a battery, acting in different time scales to assure energy and power stability, and a variable DC load that may represent electric vehicles (bus, taxi, cars) charging station.

Based on singular perturbation analysis, the system can be split in two interconnected subsystems, i.e. a fast (current) subsystem and a slow (voltage) subsystem. This induces a time scale separation that greatly simplifies the control design process, solving the non-minimum phase problem for a boost converter according to the chosen control target. It is important to remark that even though this is a current practice in industry, the formal analysis and explanation of such approach was seldom presented (see Chen et al. (2014); Iovine et al. (2017); Perez et al. (2018b)).

2. MICROGRID MODEL

A train line is integrated in the DC MicroGrid introduced in Perez et al. (2018a) to be installed in a rail (subway, train, tramway) station, where the MicroGrid is composed

of PV generation, a battery and a supercapacitor as a hybrid energy storage system and a DC load, representing the station's own needs as well as charging stations for electric vehicles (bus, taxi, car). The purpose is to allow regenerative braking, such that the surplus energy on the train electric line can be properly absorbed by the MicroGrid, avoiding overvoltage in the trains' line, and then allowing much more electric braking instead of mechanical (see Barrero et al. (2008); Dixon and Ortuzar (2002)). Fig. 1 depicts the proposed DC MicroGrid with the train line connection. The state space average model of the MicroGrid in Fig. 1 is expressed as follows:

$$\dot{V}_{C_1} = \frac{1}{R_1 C_1} V_S - \frac{1}{R_1 C_1} V_{C_1} - \frac{1}{C_1} I_{L_3} \quad (1)$$

$$\dot{V}_{C_2} = \frac{1}{R_2 C_2} V_{dc} - \frac{1}{R_2 C_2} V_{C_2} + \frac{1}{C_2} I_{L_3}(1-u_1) \quad (2)$$

$$\dot{I}_{L_3} = \frac{1}{L_3} V_{C_1} - \frac{1}{L_3} V_{C_2}(1-u_1) - \frac{R_{01}}{L_3} I_{L_3} \quad (3)$$

$$\dot{V}_{C_4} = \frac{1}{R_4 C_4} V_B - \frac{1}{R_4 C_4} V_{C_4} - \frac{1}{C_4} I_{L_6} \quad (4)$$

$$\dot{V}_{C_5} = \frac{1}{R_5 C_5} V_{dc} - \frac{1}{R_5 C_5} V_{C_5} + \frac{1}{C_5} I_{L_6}(1-u_2) \quad (5)$$

$$\dot{I}_{L_6} = \frac{1}{L_6} V_{C_4} - \frac{1}{L_6} V_{C_5}(1-u_2) - \frac{R_{04}}{L_6} I_{L_6} \quad (6)$$

$$\dot{V}_{C_7} = \frac{1}{R_7 C_7} V_{PV} - \frac{1}{R_7 C_7} V_{C_7} - \frac{1}{C_7} I_{L_9} \quad (7)$$

$$\dot{V}_{C_8} = \frac{1}{R_8 C_8} V_{dc} - \frac{1}{R_8 C_8} V_{C_8} + \frac{1}{C_8} I_{L_9}(1-u_3) \quad (8)$$

$$\dot{I}_{L_9} = \frac{1}{L_9} V_{C_7} - \frac{1}{L_9} V_{C_8}(1-u_3) - \frac{R_{08}}{L_9} I_{L_9} + \\ + \frac{1}{L_9}(R_{08} - R_{07}) I_{L_9} u_3 \quad (9)$$

$$\dot{V}_{C_{11}} = \frac{1}{R_{11} C_{11}} V_L - \frac{1}{R_{11} C_{11}} V_{C_{11}} + \frac{1}{C_{11}} I_{L_{13}} \quad (10)$$

$$\dot{V}_{C_{12}} = \frac{1}{R_{12} C_{12}} V_{dc} - \frac{1}{R_{12} C_{12}} V_{C_{12}} - \frac{1}{C_{12}} I_{L_{13}} u_4 \quad (11)$$

$$\dot{I}_{L_{13}} = -\frac{1}{L_{13}} V_{C_{11}} + \frac{1}{L_{13}} V_{C_{12}} u_4 - \frac{R_{011}}{L_{13}} I_{L_{13}} + \\ - \frac{1}{L_{13}}(R_{012} - R_{011}) I_{L_{13}} u_4 \quad (12)$$

$$\dot{V}_{C_{14}} = \frac{1}{R_{14} C_{14}} V_T - \frac{1}{R_{14} C_{14}} V_{C_{14}} - \frac{I_{L_{16}}}{C_{14}} u_5 \quad (13)$$

$$\dot{V}_{C_{15}} = \frac{1}{R_{15} C_{15}} V_{dc} - \frac{1}{R_{15} C_{15}} V_{C_{15}} + \frac{1}{C_{15}} I_{L_{16}} \quad (14)$$

$$\dot{I}_{L_{16}} = \frac{1}{L_{16}} V_{C_{14}} u_5 - \frac{1}{L_{16}} V_{C_{15}} - \frac{R_{014}}{L_{16}} I_{L_{16}} \quad (15)$$

$$\dot{V}_{dc} = \frac{1}{C_{10}} \left[\frac{V_{C_2} - V_{dc}}{R_2} + \frac{V_{C_5} - V_{dc}}{R_5} + \right. \\ \left. + \frac{V_{C_8} - V_{dc}}{R_8} + \frac{V_{C_{12}} - V_{dc}}{R_{12}} + \frac{V_{C_{15}} - V_{dc}}{R_{15}} \right] \quad (16)$$

V_S, V_B, V_{PV}, V_L and V_T are the voltages on the supercapacitor, battery, PV array, DC load and train respectively. V_{C_1}, V_{C_4}, V_{C_7}, $V_{C_{11}}$ and $V_{C_{14}}$ are the input voltages of the MicroGrid converters. I_{L_3}, I_{L_6}, I_{L_9}, $I_{L_{13}}$ and $I_{L_{16}}$ are the inductor currents in the converters, V_{C_2}, V_{C_5} , V_{C_8}, $V_{C_{12}}$ and $V_{C_{15}}$ are the output voltages of the converters. R_1, R_2, R_4, R_5, R_7, R_8, R_{11}, R_{12}, R_{14} and R_{15} are the resistances representing the cable losses, R_{01}, R_{02}, R_{04}, R_{05}, R_{07}, R_{08}, R_{011}, R_{012}, R_{014} and R_{015} are switch losses of the semiconductors. V_{dc} is the DC bus voltage and u_1, u_2, u_3, u_4 and u_5 are the modulation index of the converters in the MicroGrid.

3. CONTROL STRATEGY

3.1 Control objective

The control target is to make the following variables V_{dc}, I_{L_6}, I_{L_9}, $V_{C_{11}}$ and $V_{C_{14}}$ track their respective references V^*_{dc}, $I^*_{L_6}$, $I^*_{L_9}$, $V^*_{C_{11}}$ and $V^*_{C_{14}}$, provided by a higher control level. The voltage V^*_{dc} is a constant value designed according to the voltage level of the MicroGrid's devices, while the current $I^*_{L_6}$ is given by the calculation of the optimal power flow in the system, such saving battery's life-time. The reference $I^*_{L_9}$ is provided by the MPPT algorithm to track the maximum power point in the PV. The voltage $V^*_{C_{11}}$ is the desired voltage on the DC load chosen according to the grid requirements. Finally, the voltage $V^*_{C_{14}}$ is the desired voltage on the connection to the train to allow regenerative braking.

3.2 Control design

The system (13)-(15) consists of two interconnected subsystems [1] , i.e. the current $I_{L_{16}}$ subsystem 1 and the voltage $V_{C_{14}}$ subsystem 2. Therefore, we can develop a control such that the voltage $V_{C_{14}}$ is designed to have slower dynamics than the current $I_{L_{16}}$, resulting in a explicit time-scale separation, where the singular perturbation condition is created. With this consideration the control design can be developed separately for each subsystem.

Defining $x = V_{C_{14}}$ and $z = I_{L_{16}}$, the subsystems can be generically written as:

$$\dot{x} = f_x(x,z) + g_x(z)u \quad (17)$$

$$\dot{z} = f_z(x,z) + g_z(x)u \quad (18)$$

This system is a second order one with one control input: therefore, the remaining dynamics should be brought to the equilibrium point by the controlled one. The idea is to develop a control law where u tracks a reference trajectory x^* yet to be determined. In this case, $V^*_{C_{14}}$ is provided by the higher level control, but $I^*_{L_{16}}$ is not ready-made. Therefore, it is a crucial step to determine $I^*_{L_{16}}$, which is the desired trajectory of $I_{L_{16}}$.

Let us suppose that there is a control law $u = h(x,z)$ for the current subsystem, such that z in (18) converges to z^* as follows:

$$\dot{z} = a(z - z^*) + r(z, z^*) \quad (19)$$

where a is a positive real number and the nonlinear function r is chosen such that:

[1] The same analogy can be made for the supercapacitor system in (1)-(3).

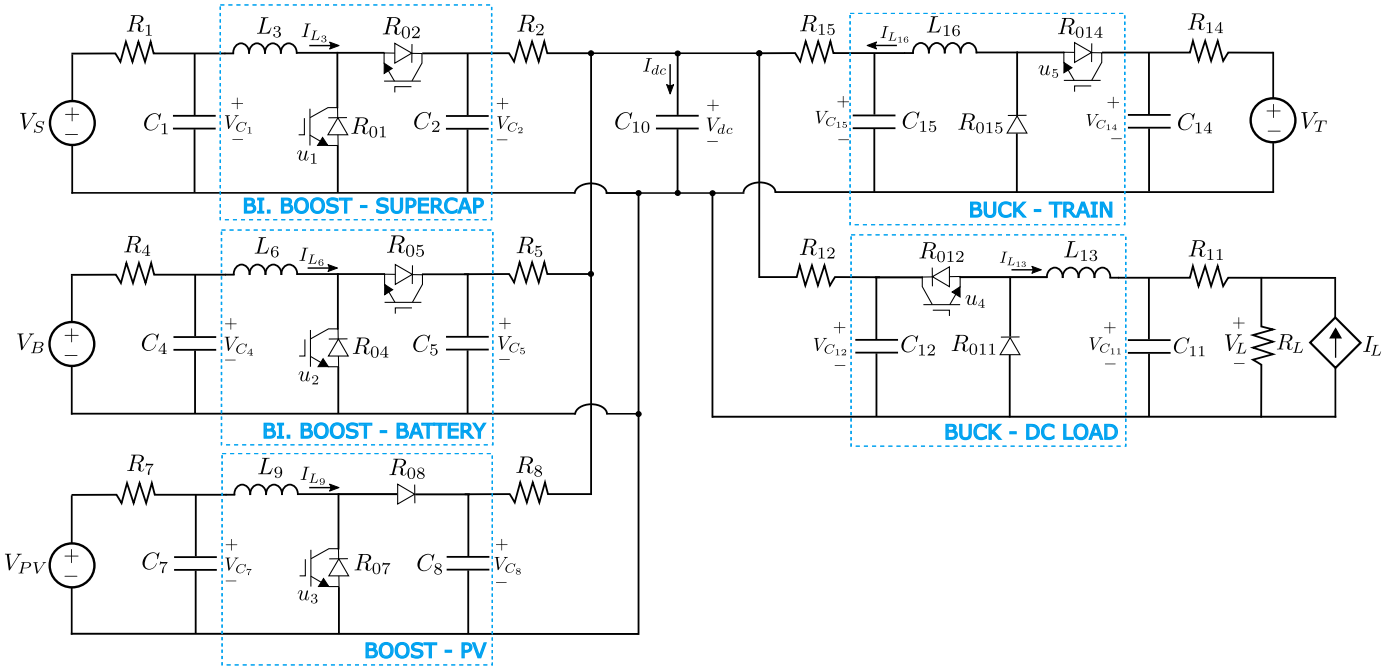

Fig. 1. The DC MicroGrid composed of a supercapacitor, a battery, a PV array, a DC load and regenerative braking from a train line.

$$\frac{||r(z,z^*)||}{||z||} \longrightarrow 0 \; as \; ||z|| \longrightarrow 0 \tag{20}$$

We can impose faster dynamics on the current subsystem designing dynamics given by constant a much faster than the voltage subsystem. Then, the control input can be written as:

$$h(x,z) = \frac{1}{g_x}[a(z-z^*) + r(z,z^*) - f_x] \tag{21}$$

where g_x must be nonsingular.

To design the voltage subsystem, let us suppose that current subsystem z is already in its equilibrium point z^* driven by (21). Hence, the control input can be written as:

$$u' = h(x,z^*) = g_z^{-1}(x,z^*) f_z(x,z^*) \tag{22}$$

Therefore, substituting $z = z^*$ and $u = u'$, we may obtain the simplified model:

$$\dot{x} = f_x(x,z^*) - g_x(x,z^*) g_z^{-1}(x,z^*) f_z(x,z^*) \tag{23}$$

The control target here is to make x steer x^*, so in (23) we use z^* to control x. Then, we suppose that exists a control law $z^* = h_2(x)$ where x can be asymptotically stabilized at x^*. We result in the following behavior:

$$\dot{x} = b(x - x^*) + r_2(x, x^*) \tag{24}$$

where b is a designed positive number and r_2 is the nonlinear part as proceeded in (20).

In order to calculate $h_2(x,z)$, we may use an additional integrator for z^* to be the control input of higher order system without zero dynamics:

$$\frac{dz^*}{dt} = v_z \tag{25}$$

where the simplified system can be written as:

$$\frac{dz}{dt} = f_x(x,z^*) - g_x(x,z^*) g_z^{-1}(x,z^*) f_z(x,z^*) \tag{26}$$

Consequently, the reference z^* can be derived via feedback linearization.

Remark: The use of singular perturbation to obtain the simplified model is valid inside an operating region that is given by the time scale ratio from the two subsystems.

3.3 Regenerative braking control

The proposed control design is now applied for the regenerative braking system of the train. Hence, u_5 can be deduced as:

$$u_5 = \frac{1}{V_{C_{14}}}\left[L_{16} v_{16} + V_{C_{15}} + R_{014} I_{L_{16}}\right] \tag{27}$$

where

$$v_{16} = \dot{I}^*_{L_{16}} - K_{16}(I_{L_{16}} - I^*_{L_{16}}) - K^{\alpha}_{16}\alpha_{16} \tag{28}$$

with $K_{16} > 0$ and $K^{\alpha}_{16} > 0$, used to regulate the speed of convergence of $I_{L_{16}}$. Then, applying the control input (27) in (13) we result in the simplified dynamics for $V_{C_{14}}$:

$$\dot{V}_{C_{14}} = \frac{V_T - V_{C_{14}}}{R_{14} C_{14}} - \frac{I^*_{L_{16}}[V_{C_{15}} + R_{015} I^*_{L_{16}}]}{C_{14} V_{C_{14}}} \tag{29}$$

Considering $V_{C_{14}}$ as the output, the calculation of its derivative until finding the control input is $v_t = \dot{I}^*_{L_{16}}$. The following Lie derivatives can be deduced:

$$\dot{V}_{C_{14}} = L^1_{f_{14}} h_{14}(x) \tag{30}$$

$$\ddot{V}_{C_{14}} = \left[\frac{V_{C_{15}} I^*_{L_{16}} + R_{015} {I^*_{L_{16}}}^2}{C_{14} {V_{C_{14}}}^2} - \frac{1}{R_{14} C_{14}}\right] \dot{V}_{C_{14}} + \tag{31}$$

$$-\frac{1}{C_{14}V_{C_{14}}}I^*_{L_{16}}\dot{V}_{C_{15}}-\frac{1}{C_{14}V_{C_{14}}}(V_{C_{15}}+2R_{015}I^*_{L_{16}})\dot{I}^*_{L_{16}}$$

$$\ddot{V}_{C_{14}}=L^2_{f_{14}}h_{14}(x)+L_{g_{14}}L^1_{f_{14}}h_{14}(x)v_t \tag{32}$$

By introducing a synthetic input θ_t, the input v_t can be designed as:

$$v_t=\frac{1}{L_{g_{14}}L^1_{f_{14}}h_{14}(x)}[\theta_t-L^2_{f_{14}}h_{14}(x)] \tag{33}$$

where the additional input is chosen using linear techniques to give the desired dynamics for $V_{C_{14}}$.

$$\theta_t=-K_{14}(\dot{V}_{C_{14}}-\dot{V}^*_{C_{14}})+K^\alpha_{14}(V_{C_{14}}-V^*_{C_{14}}) \tag{34}$$

where we can define the speed response of the voltage, using K_{14} and K^α_{14} by pole placement and $I^*_{L_{16}}$ can be easily determined by integrating $\int v_t dt = I^*_{L_{16}}$.

3.4 Supercapacitor control

The DC bus is regulated by the supercapacitor subsystem, where the power balance is given by the stability of the DC voltage: a complete stability analysis is developed to ensure asymptotic stability of the whole system. A control strategy similar to the one developed in Section 3.2 is developed for the supercapacitor subsystem.

Here, it is possible to design the current I_{L_3} to have faster dynamics than voltage V_{C_2} resulting in an explicit time-scale separation. Using singular perturbation theory, a simplified dynamics of V_{C_2} is obtained where I_{L_3} is considered already in its desired value $I^*_{L_3}$ (see Perez et al. (2018b)). Therefore, u_1 can be deduced as:

$$u_1=1+\frac{1}{V_{C_2}}\left[L_3v_3-V_{C_1}+R_{01}I_{L_3}\right] \tag{35}$$
$$v_3=\dot{I}^*_{L_3}-K_3(I_{L_3}-I^*_{L_3})-K^\alpha_3\alpha_3$$

with positive K_3 and K^α_3 which are used to regulate the convergence speeds of I_{L_3}. Then, applying the control input (35) in (2) results in simplified dynamics for V_{C_2}:

$$\dot{V}_{C_2}=\frac{1}{R_2C_2}(V_{dc}-V_{C_2})+\frac{I^*_{L_3}}{C_2V_{C_2}}[V_{C_1}-R_{01}I^*_{L_3}] \tag{36}$$

The following Lie derivatives can be then deduced:

$$\dot{V}_{C_2}=L^2_{f_2}h_2(x) \tag{37}$$
$$\ddot{V}_{C_2}=L^2_{f_2}h_2(x)+L_{g_2}L^1_{f_2}h_2(x)v_d \tag{38}$$

The chosen control input is $v_d=\dot{I}^*_{L_3}$, therefore we have full state transformation with no zero dynamics:

$$v_d=\frac{V_{C_2}}{V_{C_1}-2R_{01}I^*_{L_3}}\left[C_2v_2-\frac{\dot{V}_{dc}}{R_2}-\frac{I^*_{L_3}}{V_{C_2}}\dot{V}_{C_1}+\right.$$
$$\left.+\dot{V}_{C_2}\left(\frac{1}{R_2}+\frac{V_{C_1}I^*_{L_3}-R_{01}{I^*_{L_3}}^2}{{V_{C_2}}^2}\right)\right] \tag{39}$$
$$v_2=-K_2(\dot{V}_{C_2}-\dot{V}^*_{C_2})+K^\alpha_2(V_{C_2}-V^*_{C_2}) \tag{40}$$

We can define the speed of convergence for V_{C_2}, allocating the gains by pole placement to get slower voltage dynamics for the simplified model (see Perez et al. (2018a)).

3.5 Stability Analysis

We may propose a Lyapunov function W to perform calculations of the reference $V^*_{C_2}$ such that V_{dc} is stabilized in V^*_{dc}. The Lyapunov function is composed by the interconnection voltages of the MicroGrid to ensure stability of those variables.

$$W=\frac{C_{10}}{2}V^2_{dc}+\frac{C_5}{2}(V_{C_5}-V^e_{C_5})^2+\frac{C_8}{2}(V_{C_8}-V^e_{C_8})^2$$
$$+\frac{C_{12}}{2}(V_{C_{12}}-V^e_{C_{12}})^2+\frac{C_{15}}{2}(V_{C_{15}}-V^e_{C_{15}})^2 \tag{41}$$

The derivative of W can be calculated as follows, where V_{C_2} is the degree of freedom used as the control input:

$$\dot{W}=V_{dc}\left[\frac{V^*_{C_2}-V_{dc}}{R_2}+\frac{V_{C_5}-V_{dc}}{R_5}+\right.$$
$$\left.+\frac{V_{C_8}-V_{dc}}{R_8}+\frac{V_{C_{12}}-V_{dc}}{R_{12}}+\frac{V_{C_{15}}-V_{dc}}{R_{15}}\right]+$$
$$+(V_{C_5}-V^e_{C_5})\left[\frac{1}{R_5}(V_{dc}-V_{C_5})+I_{L_6}(1-u_2)\right]+$$
$$+(V_{C_8}-V^e_{C_8})\left[\frac{1}{R_8}(V_{dc}-V_{C_8})+I_{L_9}(1-u_3)\right]+$$
$$+(V_{C_{12}}-V^e_{C_{12}})\left[\frac{V_{dc}-V_{C_{12}}}{R_{12}}-I_{L_{13}}u_4\right]+$$
$$+(V_{C_{15}}-V^e_{C_{15}})\left[\frac{V_{dc}-V_{C_{15}}}{R_{15}}+I_{L_{16}}\right] \tag{42}$$

In order to obtain asymptotic stable behavior, we investigate the time derivative of W (see Khalil (2014)), where a desired stable expression for $\dot{W}$ can be written as:

$$\dot{W}=-\frac{(V^2_{dc}-{V^*_{dc}}^2)}{R_2}-\frac{(V_{C_5}-V^e_{C_5})^2}{R_5}+$$
$$-\frac{(V_{C_8}-V^e_{C_8})^2}{R_8}-\frac{(V_{C_{12}}-V^e_{C_{12}})^2}{R_{12}}-\frac{(V_{C_{15}}-V^e_{C_{15}})^2}{R_{15}} \tag{43}$$

The control input V_{C_2} is obtained from expression (43) and can be expressed as:

$$V^*_{C_2}=\frac{R_2}{V_{dc}}\left\{\frac{1}{R_2}{V^*_{dc}}^2-V_{dc}\left[\frac{V_{C_5}-V_{dc}}{R_5}+\right.\right.$$
$$\left.+\frac{V_{C_8}-V_{dc}}{R_8}+\frac{V_{C_{12}}-V_{dc}}{R_{12}}+\frac{V_{C_{15}}-V_{dc}}{R_{15}}\right]+$$
$$-(V_{C_5}-V^e_{C_5})\left[\frac{1}{R_5}(V_{dc}-V^e_{C_5})+I_{L_6}(1-u_2)\right]+$$
$$-(V_{C_8}-V^e_{C_8})\left[\frac{1}{R_8}(V_{dc}-V^e_{C_8})+I_{L_9}(1-u_3)\right]+$$
$$-(V_{C_{12}}-V^e_{C_{12}})\left[\frac{V_{dc}-V_{C_{12}}}{R_{12}}-I_{L_{13}}u_4\right]+$$
$$-(V_{C_{15}}-V^e_{C_{15}})\left[\frac{V_{dc}-V_{C_{15}}}{R_{15}}+I_{L_{16}}\right]+$$
$$-\frac{(V_{C_5}-V^e_{C_5})^2}{R_5}-\frac{(V_{C_8}-V^e_{C_8})^2}{R_8}+$$
$$\left.-\frac{(V_{C_{12}}-V^e_{C_{12}})^2}{R_{12}}-\frac{(V_{C_{15}}-V^e_{C_{15}})^2}{R_{15}}\right\} \tag{44}$$

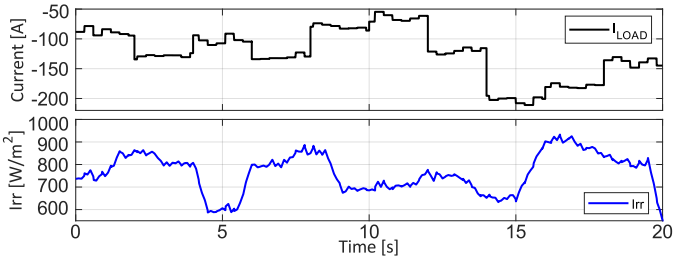

Fig. 2. DC load current and solar irradiation.

The Lyapunov function in (41) results to be a ISS-like Lyapunov function, where V_{dc}^{*} is playing the role of a virtual input (see Iovine et al. (2018); Sontag (2008); Krommydas and Alexandridis (2015)).

The control strategy for the battery, PV system and the DC load are not presented here for lack of space, but the control law of these systems are developed in Perez et al. (2018a).

4. SIMULATION RESULTS

The proposed DC MicroGrid is implemented on *Matlab/Simulink* to study the performance of the control strategy developed in this paper. The supercapacitor has 50 F with 400 V of nominal voltage, resulting in 720 kW nominal power rate. The lithium-ion battery has 150 kW of nominal power with nominal voltage of 380 V. The secondary controller allocates the battery to have a piecewise constant variation to save its life cycle. The PV array is composed of 200 parallel cells and 15 series cells of 60 W, resulting in 180 kWp of nominal power. The MPPT algorithm used is the incremental conductance one. The train has nominal voltage of 750 V, but during the braking period the voltages increases very fast up to 800 V, which results in a burst of power about 400 kW into the MicroGrid. The DC load varies according to the power demand with 100 kW of maximum consumption. The load is supplied with 500 V. The DC/DC converters work with 10 kHz of switching frequency. Table 1 introduces the DC MicroGrid parameters used on simulations.

Table 1. MicroGrid parameters

Cap	Battery	PV	DC load	Train	Value
R_1	R_4	R_7	R_{11}	R_{14}	0.1 Ω
C_1	C_4	C_7	C_{11}	C_{14}	1 mF
R_2	R_5	R_8	R_{12}	R_{15}	0.1 Ω
C_2	C_5	C_8	R_{12}	C_{15}	10 mF
L_3	L_6	L_9	R_{13}	L_{16}	3.3 mH
R_{01}	R_{04}	R_{07}	R_{011}	R_{015}	10 $m\Omega$
R_{02}	R_{05}	R_{08}	R_{014}	R_{014}	10 $m\Omega$

Fig. 2 depicts the variations on load current and solar irradiation, used as simulation's inputs to bring the DC MicroGrid into nonlinear operating regions. The voltages V_S, V_B, V_{PV} and V_T are introduced in Fig. 3. The supercapacitor voltage V_S varies to regulate the mismatch of power in the DC bus assuring voltage stability. The battery is controlled with piecewise constant behavior to provide power flow regulation in long term and the PV voltage varies according to the irradiation profile. The voltage on the train V_T remains constant in 750 V but during the regenerative braking period the voltage increases up to 800 V.

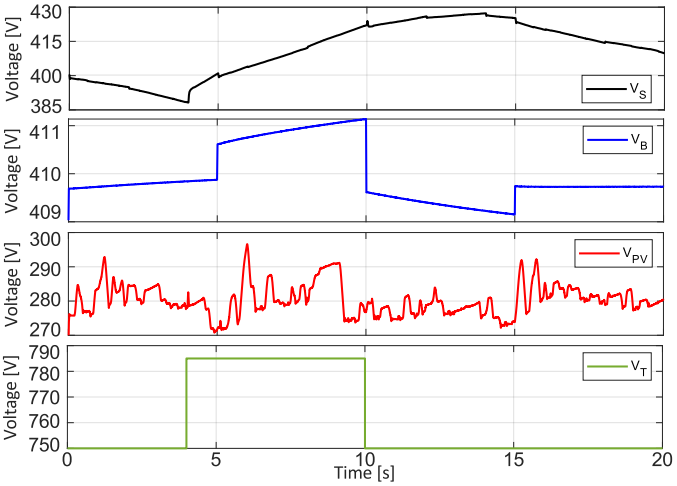

Fig. 3. Voltages V_S, V_B, V_{PV} and V_T respectively.

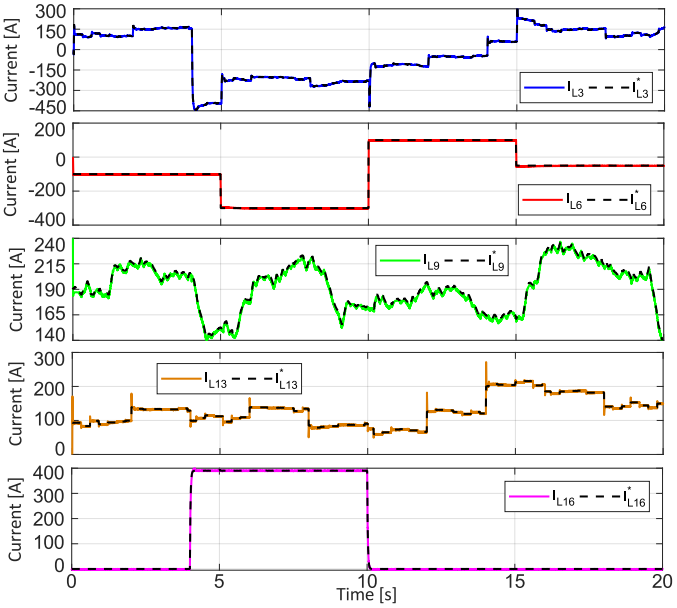

Fig. 4. Currents I_{L_3}, I_{L_6}, I_{L_9}, $I_{L_{13}}$ and $I_{L_{16}}$ respectively.

Fig. 4 introduces currents I_{L_3}, I_{L_6}, I_{L_9}, $I_{L_{13}}$ and $I_{L_{16}}$ with their respective control references. It can be seen that the supercapacitor operates in fast dynamics to provide the stability of the DC voltage. Reference $I_{L_3}^{*}$ is continuously varying to correct grid's power mismatch. The battery current I_{L_6} follows its reference given by a higher control level to slowly balance the power flow in the system. Currents I_{L_9} and $I_{L_{13}}$ varies according to the nonlinear behavior of PV and DC load. The currents $I_{L_{16}}$ reacts only during the regenerative braking period.

Figures 5 and 6 depict the voltages. The voltage V_{C_2} is the control input selected in the supercapacitor subsystem to stabilize the DC bus voltage. The voltage on the DC bus V_{dc} is controlled in a constant reference $V_{dc} = 630$ V, such that the balance of power is guaranteed, allowing each device of the system (Battery, PV, DC load and train) operate according to their control targets. The voltage V_{dc} is properly controlled, where the voltage presents fast control response with good control performance. Therefore, it is possible to accomplish the target to correctly feed the DC load, where the voltage is controlled in the reference $V_{C_{11}^{*}}$

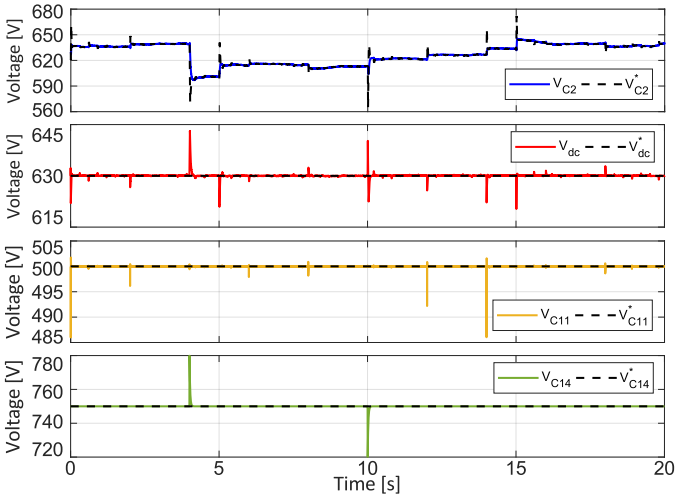

Fig. 5. Voltage V_{C_2} on supercapacitor's converter and DC bus voltage V_{dc}.

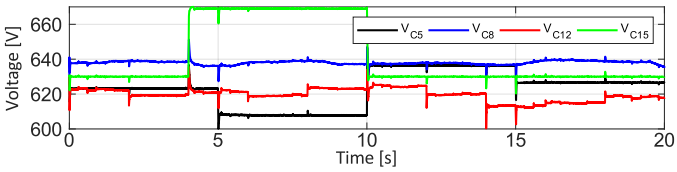

Fig. 6. Voltages V_{C_5}, V_{C_7}, V_{C_8}, $V_{C_{12}}$ and $V_{C_{15}}$.

with small transient variations. Finally, the voltage $V_{C_{14}}$ on the train is controlled to allow the power generated by the regenerative braking to be injected into the MicroGrid. In the regenerative braking, the voltage of the train V_T increases and the difference of voltage between V_T and $V_{C_{14}}$ allows the current flows into the MicroGrid, where this fast peak of power is absorbed by the supercapacitor. Fig. 6 introduces the remaining dynamics of the system, voltages V_{C_5}, V_{C_7}, V_{C_8}, $V_{C_{12}}$ and $V_{C_{15}}$. They are the systems' zero dynamics and according to the figure they have stable behavior going to their equilibrium points.

5. CONCLUSION

This paper proposes a control strategy to allow regenerative braking power injection of a train line into a DC MicroGrid while ensuring system stability. The supercapacitor's target is to balance the power mismatch, mainly due to the power burst caused by the train braking, while the battery provides power flow regulation in long term. The control scheme is based on singular perturbation theory, where the system can be synthetically split in two subsystems with different time-scale. The stability of the systems is guaranteed with a strategy that greatly simplifies the control design. Simulations of the whole system highlight the control performance of the MicroGrid with the regenerative train braking.

REFERENCES

R. Barrero, J. V. Mierlo, and X. Tackoen. Energy savings in public transport. *IEEE Vehicular Technology Magazine*, 3(3):26–36, Sept 2008. ISSN 1556-6072. doi: 10.1109/MVT.2008.927485.

Y. Chen, G. Damm, A. Benchaib, M. Netto, and F. Lamnabhi-Lagarrigue. Control induced explicit time-scale separation to attain dc voltage stability for a vsc-hvdc terminal. In *IFAC Proceedings Volumes (IFAC-PapersOnline)*, volume 19, 08 2014.

J. W. Dixon and M. E. Ortuzar. Ultracapacitors + dc-dc converters in regenerative braking system. *IEEE Aerospace and Electronic Systems Magazine*, 17(8):16–21, Aug 2002. ISSN 0885-8985. doi: 10.1109/MAES.2002.1028079.

J. C. Hernandez and F. S. Sutil. Electric vehicle charging stations feeded by renewable: Pv and train regenerative braking. *IEEE Latin America Transactions*, 14(7):3262–3269, July 2016. ISSN 1548-0992. doi: 10.1109/TLA.2016.7587629.

A. Iovine, S. B. Siad, G. Damm, Elena De Santis, and M. D. Di Benedetto. Nonlinear Control of a DC MicroGrid for the Integration of Photovoltaic Panels. *IEEE Transactions on Automation Science and Engineering*, 14(2):524–535, April 2017. ISSN 1545-5955. doi: 10.1109/TASE.2017.2662742.

A. Iovine, G. Damm, E. De Santis, M. D. Di Benedetto, L. Galai-Dol, and P. Pepe. Voltage Stabilization in a DC MicroGrid by an ISS-like Lyapunov Function implementing Droop Control. In *ECC 2018 - European Control Conference*, Jun 2018.

Hassan K Khalil. *Nonlinear control*. Prentice Hall, 2014.

K. F. Krommydas and A. T. Alexandridis. Modular Control Design and Stability Analysis of Isolated PV-Source/Battery-Storage Distributed Generation Systems. *IEEE Journal on Emerging and Selected Topics in Circuits and Systems*, 5(3):372–382, Sept 2015. ISSN 2156-3357. doi: 10.1109/JETCAS.2015.2462172.

S. Lu, P. Weston, S. Hillmansen, H. B. Gooi, and C. Roberts. Increasing the regenerative braking energy for railway vehicles. *IEEE Trans. on Intelligent Transportation Systems*, 15(6):2506–2515, Dec 2014. ISSN 1524-9050. doi: 10.1109/TITS.2014.2319233.

D. E. Olivares, A. Mehrizi-Sani, A. H. Etemadi, C. A. Caizares, R. Iravani, M. Kazerani, A. H. Hajimiragha, O. Gomis-Bellmunt, M. Saeedifard, R. Palma-Behnke, G. A. Jimnez-Estvez, and N. D. Hatziargyriou. Trends in microgrid control. *IEEE Transactions on Smart Grid*, 5(4):1905–1919, July 2014. ISSN 1949-3053. doi: 10.1109/TSG.2013.2295514.

F. Perez, G. Damm, F. Lamnabhi-Lagarrigue, and P. Ribeiro. Nonlinear Control for Isolated DC MicroGrids. *Revue Africaine de la Recherche en Informatique et Mathématiques Appliquées*, 30, 2018a.

F. Perez, A. Iovine, G. Damm, and P. Ribeiro. DC microgrid voltage stability by dynamic feedback linearization. In *2018 IEEE International Conference on Industrial Technology (ICIT)*, pages 129–134, Feb 2018b. doi: 10.1109/ICIT.2018.8352164.

P. F. Ribeiro, H. Polinder, and M. J. Verkerk. Planning and designing smart grids: Philosophical considerations. *IEEE Technology and Society Magazine*, 31(3):34–43, Fall 2012. ISSN 0278-0097. doi: 10.1109/MTS.2012.2211771.

Paulo F Ribeiro, Brian K Johnson, Mariesa L Crow, Aysen Arsoy, and Yilu Liu. Energy storage systems for advanced power applications. *Proceedings of IEEE*, 89, 2001.

Eduardo D Sontag. Input to state stability: Basic concepts and results. In *Nonlinear and optimal control theory*, pages 163–220. Springer, 2008.